Full length article

Density functional study of the adsorption of NO on Ni_n (n = 1, 2, 3 and 4) clusters doped functionalized graphene support

Zhengyang Gao[a], Ang Li[a],*, Xiaoshuo Liu[a], Chuanzhi Ma[a], Xiang Li[a], Weijie Yang[a],*, Xunlei Ding[b]

[a] School of Energy and Power Engineering, North China Electric Power University, Baoding 071003, China
[b] School of Mathematics and Physics, North China Electric Power University, Beijing 102206, China

ARTICLE INFO

ABSTRACT

Density functional theory calculations were used to study the adsorption of NO on Ni_n cluster (n = 1, 2, 3 and 4) doped graphene with different graphene-based support (single vacancy, one nitrogen decorated, two nitrogen decorated and three nitrogen decorated). The adsorption configuration, adsorption energy, charge transfer, density of states of NO on Ni_n/graphene are thoroughly studied. In addition, the d-band center and Fermi softness have been performed to consider the support effect. It is found that the support effect has a significant effect on the adsorption characteristics of NO molecule, which depends on the electronic structure of graphene-based support. The electronic structure can be characterized by the Fermi softness of the catalyst. Ni atom plays a more and more obvious role in NO adsorption process, with the increase of the number of Ni atoms. The Fermi softness is a great descriptors for the adsorption activity of the Ni_n/graphene. This result can contribute to the systematic study of graphene catalysts supported on metal clusters.

1. Introduction

NO is one of the main pollutants in coal-fired power plants, which not only cause acid rain, photochemical smog and haze but also bring a risk for human and animals because prolonged exposure to Nitrogen oxides will cause cardiac dysfunctions and respiratory symptoms [1]. In order to eliminate the harm caused by NO, the power plant mainly adopts selective catalytic reduction with ammonia injection (NH_3-SCR) technology [2–4]. Although the NH_3-SCR technology can effectively reduce NO emissions to a reasonable range. There are still some problems in the operation process. Power plant consumes a large amount of ammonia to ensure efficient NO removal, which can cause catalyst poisoning [5] and ammonia slipping [6]. In addition, the catalytic efficiency of NH_3-SCR is related to temperature and the removal efficiency NO of NH_3-SCR under low temperature is relatively low, which may cause that nitrogen removal cannot reach the environmental standard [7,8]. However, catalytic oxidation of NO to NO_2 can avoid the disadvantages of NH_3-SCR, because NO_2 can be well absorbed by desulphurizing slurry in wet flue gas desulfurization system (WFGD) through utilizing its good water solubility [9]. So catalytic oxidation is a promising technology to reduce NO under low temperature and without ammonia spillover. However, such efficient catalyst has yet been produced. So developing a new and efficient catalyst is the key to solve this problem.

Metal nanoparticles are commonly used for nanocatalysis due to its good catalytic effect. So the catalytic properties of metal nanoparticles have been widely studied. Dobrin et al. [10] investigated the CO oxidation on Pt nanoclusters of approximately 1 nm in size by using density functional theory (DFT) and found that the Pt clusters of larger size have better oxidation effect than the smaller Pt clusters. Guo et al. [11] calculated CO oxidation on subnanometer Al-Pt_n clusters and found that mixing two different metals (Al and Pt) can facilitate the occurrence of catalytic reaction. Lian et al. [12] investigated the reaction mechanism of CO oxidation catalyzed by several Pt_3M (M = Pt, Ni, Mo, Ru, Pd, Rh) clusters and found that Pt_3Mo exhibits good catalytic activity for CO oxidation. Weiss et al. [13] studied the reaction mechanism of Pt clusters for catalytic oxidation of NO gas and found that NO_2 inhibited the oxidation of NO. But there is little research on the catalysis of Ni clusters, so Ni clusters were chosen in this work.

Graphene, with its unique electrical properties, mechanical properties, thermal properties, optical properties and high specific surface area, not only has been widely used in conductive switching [14], bioimaging [15] and detector [16], but also has become an excellent support for metal nanomaterials [17–20]. Koizumi et al. [21] studied the oxidation of CO on Al-Pt alloy clusters/graphene and found that the catalyst can maintain good catalytic efficiency at room temperature. Tang et al. [22] studied the oxidation process of CO on graphene doped Pt clusters and found that the catalytic properties of functionalized
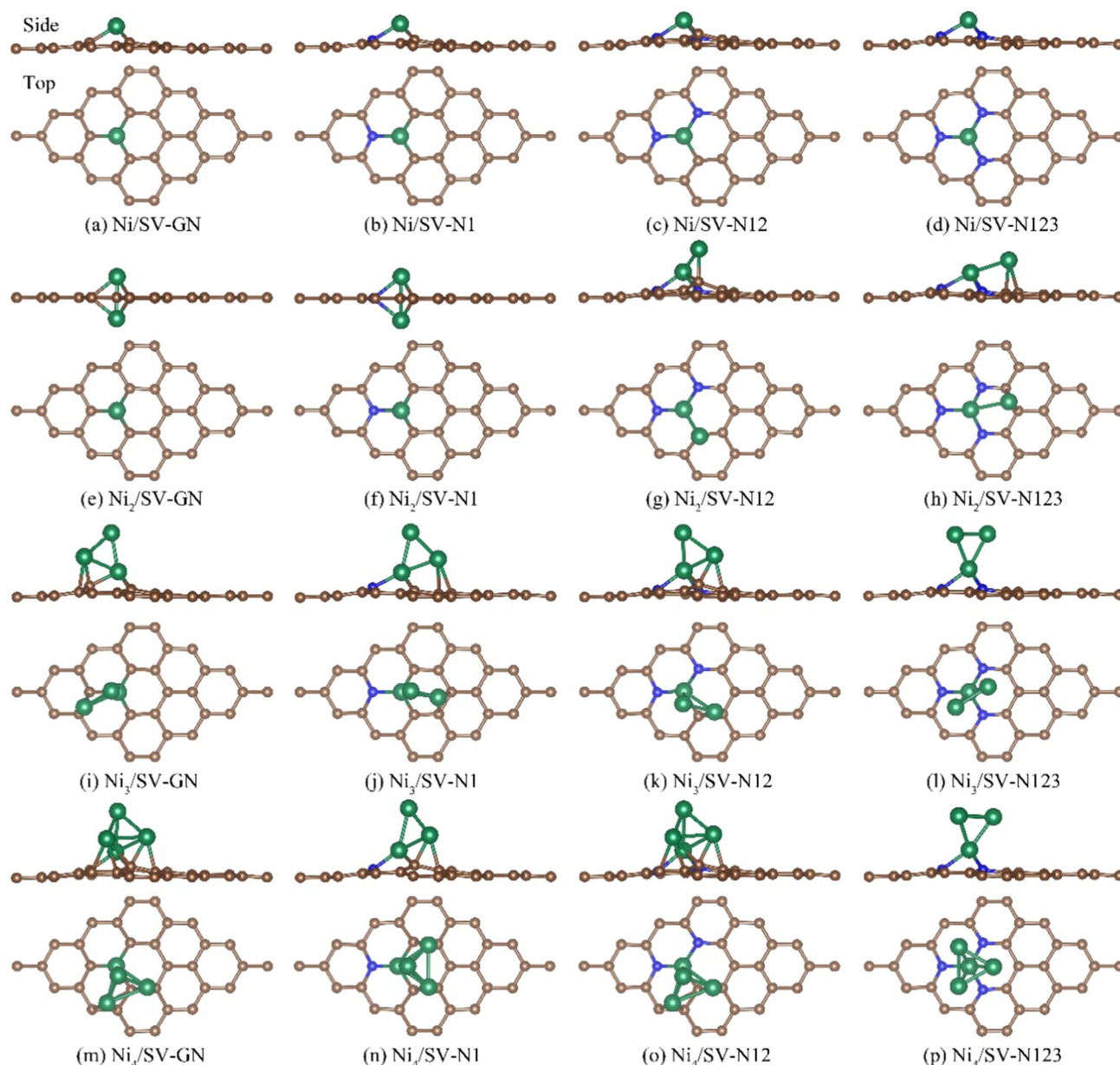
Fig. 1. The lowest-energy geometry structures of Ni clusters on single vacancy and doping different N atoms graphene. (Brown, blue and green ball represents carbon nitrogen and nickel atom).

graphene-Pt clusters catalyzer is better than pristine graphene-Pt clusters catalyzer. So we hope that graphene doped Ni clusters can play a very obvious role in the catalytic oxidation of NO, but there is no study of the catalytic oxidation of NO on graphene doped Ni clusters. Adsorption is the basis of catalytic reactions. Nowadays, many researchers have studied the adsorption of gas molecules on Ni clusters/graphene. The hydrogen molecule adsorbed on Ni clusters/graphene is studied in the previous research and it is found that hydrogen is adsorbed on the catalyst in the form of dissociation adsorption and the catalyst is a good catalyst for hydrogenation reaction [23,24]. Xu et al. [25] studied the adsorption of CO_2 on Ni_4 cluster and Ni_4/MGr and found that the adsorption effect on Ni_4/MGr is better than that on Ni_4 cluster. So the adsorption of NO on Ni cluster/graphene is the emphasis of this work. In order to avoid aggregation of Ni nanocluster caused by weak interaction between Ni clusters and graphene, Robertson et al. [26] showed that focused electron beam irradiation has been used to create mono and divacancy in graphene within a defined area, which those vacancies can be used as a fixed site for Ni clusters. The single vacancy is composed of a C atom removed from graphene, and the double vacancy is composed of two C atom removed from graphene. Previous studies have shown that single vacancy increases the surface instability of graphene [27,28]. The N-doped graphene not only possess the characteristics of excellent graphene carriers but also shows some unique properties [29]. So single vacancy, single vacancy decorated one nitrogen atom, single vacancy decorated two nitrogen atom and single vacancy decorated three nitrogen atom is chosen as the graphene-based supports to doped the Ni_n clusters, which are denoted as Ni_n/SV-GN, Ni_n/SV-N1, Ni_n/SV-N12 and Ni_n/SV-N123.

In this work, density functional theory calculations were used to investigate the adsorption of NO gas molecule on Ni_n cluster doped graphene with different graphene-based support (Ni_n/SV-GS). Firstly, the most stable geometries of Ni_n cluster doped different graphene-based support were calculated to prepare for the adsorption of NO. Secondly, the most stable adsorption geometry and the adsorption energy of the NO gas molecule on Ni_n/SV-GS ($n = 1, 2, 3$ and 4) were calculated to identify the adsorption type and the adsorption energy.

Table 1
The binding energy of Ni clusters and graphene (E$_b$, eV), the adsorption height of the Ni clusters (h, Å), the charge of the Ni$_1$ (q$_1$, e) and the bond length of Ni−Ni bonds (d$_{Ni-Ni}$, Å) of each geometries.

Ni$_n$/SV-GS	E$_b$	Δh	q$_1$	d$_{Ni-Ni}$
Ni/SV-GN	−6.691	1.247	9.501	\
Ni/SV-N1	−5.363	1.255	9.397	\
Ni/SV-N12	−5.004	1.403	9.298	\
Ni/SV-N123	−4.320	1.364	9.227	\
Ni$_2$/SV-GN	−8.046	1.200	9.538	2.402
Ni$_2$/SV-N1	−5.839	1.248	9.474	2.512
Ni$_2$/SV-N12	−4.879	1.330	9.393	2.215
Ni$_2$/SV-N123	−3.655	1.410	9.350	2.323
Ni$_3$/SV-GN	−6.628	1.408	9.578	2.245
Ni$_3$/SV-N1	−5.168	1.356	9.495	2.265
Ni$_3$/SV-N12	−5.167	1.454	9.447	2.241
Ni$_3$/SV-N123	−4.219	1.478	9.414	2.241
Ni$_4$/SV-GN	−6.973	1.456	9.578	2.359
Ni$_4$/SV-N1	−5.747	1.506	9.473	2.337
Ni$_4$/SV-N12	−5.563	1.441	9.457	2.349
Ni$_4$/SV-N123	−4.437	1.481	9.459	2.286

Thirdly, The electron density difference and the density of states of NO and Ni$_n$/SV-GS system were drawn to obtain the adsorption characteristics of this system. Ultimately, the relationship between adsorption activity and graphene-based support was further understood by studying the d-band center and Fermi softness of Ni$_n$/SV-GS catalyst. This work can provide a more in-depth and systematic understanding of cluster doped graphene-based support catalysts and play a guiding role in the design of catalysts for gas adsorption.

2. Method

All the calculations were carried out with the Vienna ab initio simulation package (VASP) based on density functional theory (DFT) [30–32]. The generalized gradient approximation (GGA) with the Perdew-Burke-Ernzerhof (PBE) function was adopted to describe electron exchange and correlation [33,34]. Similar to single atom catalysts [35–37], all calculations were carried out on 4 × 4 single layer graphene consisting of 32 carbon atoms. In order to avoid the interaction of mirror images, the thickness of the vacuum layer was in excess of 15 Å.

All calculations were performed on the plane-wave basis set with the kinetic energy cutoff of 500 eV, and the Gaussian smearing width was selected 0.05 eV. The positions of all atoms were allowed to fully relax with the conjugate gradient method for structure optimization, and the force on any atoms was < 0.02 eV/Å. Considering the computational time and accuracy, the Brillouin zone was sampled with a 7 × 7 × 1 Γ-centered k-point grid for structure optimization calculation, and the k-point grid selection was tested until the energy change was < 10 meV per atom, while a 15 × 15 × 1 Γ-centered k-point grid was used to calculate the energy and density of states (DOS). For the structure optimization and DOS calculation, the total energy convergence precision was set to be 10^{-5} eV. The optimized C−C bonds are 1.417 Å, which is consistent with the results calculated by previous theoretical studies. (d$_{C-C}$ = 1.420 Å) [38].

The binding energies (E$_b$) of Ni$_n$ (n = 1–4) nanocluster and substrates were calculated as follows:

$$E_b = E_{sub+Ni_n} - E_{sub} - E_{Ni_n} \tag{1}$$

where E_{sub+Ni_n}, E_{sub} and E_{Ni_n} represent the total energy of Ni$_n$/SV-GS, graphene substrates and Ni$_n$ (n = 1–4) nanoclusters, respectively.

The adsorption energies (E$_{ad}$) is as a metric for the interaction strength between the NO gas and graphene substrates doped Ni$_n$ (n = 1–4) nanoclusters, which were defined as follows:

$$E_{ad} = E_{NO-sub+Ni_n} - E_{sub+Ni_n} - E_{NO} \tag{2}$$

where $E_{NO-sub+Ni_n}$, E_{sub+Ni_n} and E_{NO} represent the total energy of the graphene-Ni$_n$-NO system, the total energy Ni$_n$/GS and the energy of NO gas, respectively. The NO molecule as obtained from DFT calculations. As the defined here, the more negative values of E$_{ad}$, the stronger adsorption strength.

The cohesive energies (E$_{coh}$) [39] of Ni$_n$ clusters (n = 1, 2, 3 and 4) were defined as follows:

$$E_{coh} = (E_{Ni_n} - n \cdot E_{Ni})/n \tag{3}$$

where E_{coh}, E_{Ni} and n represent the total energies of Ni$_n$ cluster, the total energies of isolated Ni atoms in the gas phase, and the number of Ni atoms in the Ni$_n$ cluster, respectively. E$_{coh}$ is mainly used to determine whether atoms are reunited.

3. Result and discussion

3.1. Catalyst model

In order to obtain the most stable structure of Ni$_n$ (n = 1, 2, 3 and 4) anchored on single vacancy and doping different N atoms graphene, we built many adsorption configurations. Through calculation, we selected sixteen the most stable structures for the research, as shown in Fig. 1. According to the number of vacancies in graphene, we divide Ni$_n$/SV-GS into four groups, the first is one Ni atom with single vacancy graphene-based substrates (Ni/SV-GS), the second is two Ni atoms with single vacancy graphene-based substrates (Ni$_2$/SV-GS), the third is three Ni atoms with single vacancy graphene-based substrates (Ni$_3$/SV-GS), the last is four Ni atoms with single vacancy graphene-based substrates (Ni$_4$/SV-GS). In Fig. 1, the number of nitrogen atoms in Ni/SV-GS increases gradually from Fig. 1(a) to (d); the number of nitrogen atoms in Ni$_2$/SV-GS increases gradually from Fig. 1(e) to (h); the number of nitrogen atoms in Ni$_3$/SV-GS increases gradually from Fig. 1(i) to (l); the number of nitrogen atoms in Ni$_4$/SV-GS increases gradually from Fig. 1(m) to (p). The binding energy of Ni clusters and graphene system, the distance between the most closed to graphene of Ni clusters and graphene, the charge of the Ni$_1$ atom and the bond length of Ni−Ni bonds are shown in Table 1.

The Ni$_n$/SV-GN and Ni$_n$/SV-N123 (n = 1, 2, 3 and 4) catalyst has been studied [25,38]. The calculated structural parameters of Ni$_n$/SV-GN and Ni$_n$/SV-N123 catalysts in this work correspond well with the previous results, which prove the correctness and rationality of the calculation in this paper. In previous studies, the stability is a key factor for single atom catalysts. The laws of single atoms are used in clusters. Xu et al. [25] has been studied the Ni$_n$ clusters on the original graphene, concluded that the binding energy of Ni$_n$ (n = 1–4) on the original graphene is −0.73 eV, −1.52 eV, −1.73 eV, −1.97 eV, which is much smaller than that of the single vacancy doped different nitrogen atoms graphene. It is indicated that the binding energy of Ni$_n$/SV-GS (n = 1, 2, 3 and 4) is very large to anchor the Ni cluster. To further illustrate the stability of Ni clusters, the concept of cohesive energy will be introduced as a reference. The cohesive energies of Ni$_n$ clusters are −1.418 eV, −1.839 eV and −2.146 eV, respectively, which is smaller than the binding energy of Ni$_n$/SV-GS (n = 2, 3 and 4). As mentioned above, Ni atoms will not reunite, so Ni$_n$ clusters have better stability.

By comparing Ni clusters four structures, we can find that with the increase of the number of nitrogen atoms, the binding energy E$_b$ of Ni and graphene-based substrates system decreases, from −6.691 eV (SV/GN), −5.363 eV (SV/N1), −5.004 eV (SV/N12) to −4.320 eV (SV/N123). Other Ni$_n$ clusters structures have the similar laws. By observing the binding energy of all graphene-based supports, we can find that the binding energy varies greatly with different substrates, which suggested that the support effect of graphene-based supports has important influence on the stability of the Ni$_n$ clusters.

In Fig. 1, it is found that one Ni atom of Ni clusters can strongly trapped in the threefold cavity (the single vacancy) on those sixteen substrate monolayer. It's found that the distance between the Ni atom in
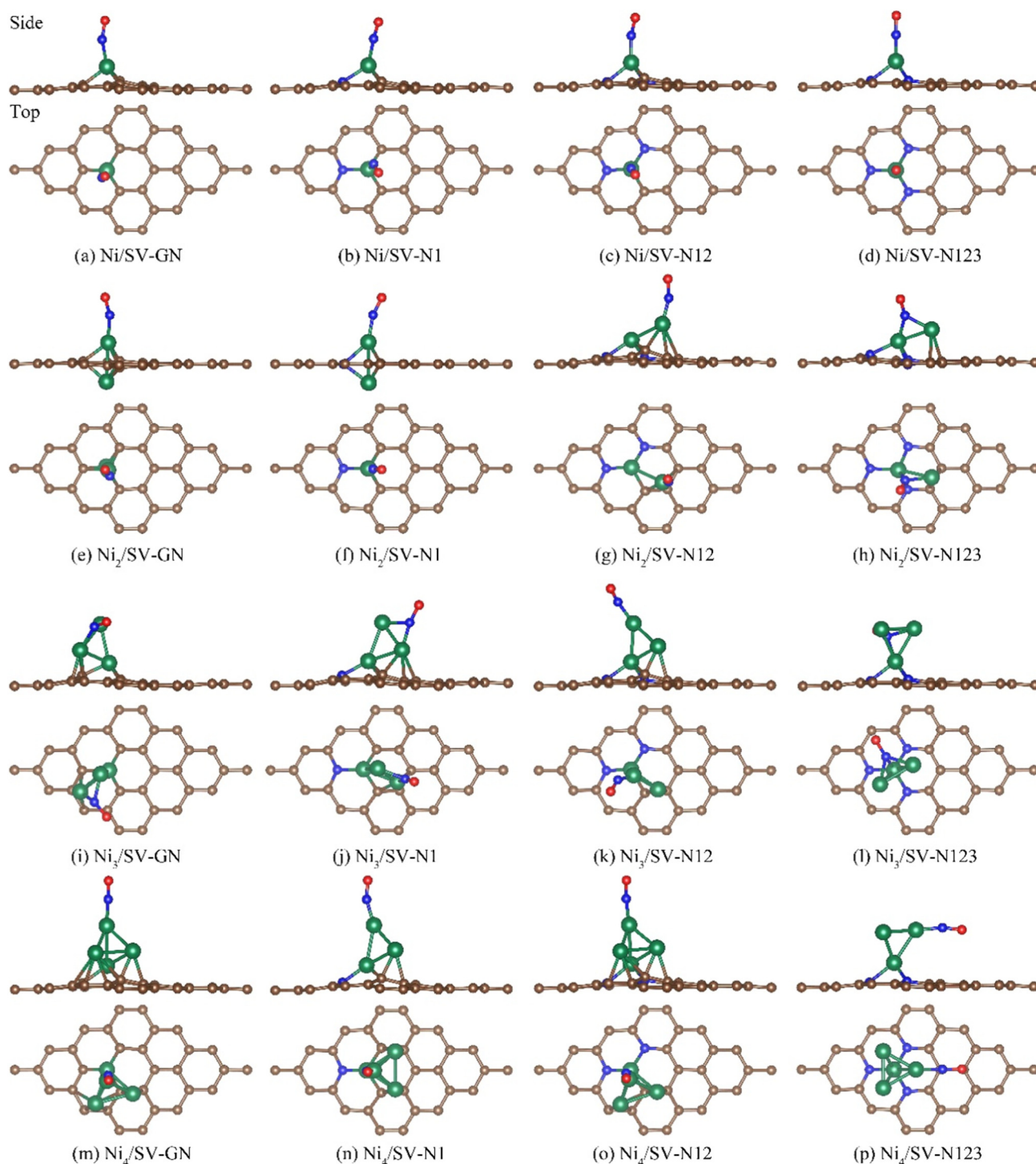
Fig. 2. The geometry structures of NO molecule adsorb on Ni_n/SV-GS. (Brown, blue, green and red ball represents carbon, nitrogen, nickel and oxygen atom).

the Ni cluster closest to the graphene substrate and substrate monolayer is about 1.2–1.5 Å. Ramos-Castillo et al. [39] calculated that the bond lengths of Ni−Ni bonds for isolated Ni_n clusters (n = 2–4) are 2.12 Å, 2.24 Å and 2.31 Å respectively. Compared with Ni clusters doped on graphene (as shown in Table 1), it can be found that the bond length of Ni clusters doped on graphene is longer than isolated Ni_n clusters (n = 2–4). In other words, Ni clusters doped on graphene will make the Ni−Ni bond of Ni cluster elongated. It is indicated that the catalytic activity of metal nanoclusters further improved by graphene-based supports. In the research of Zhou et al. [38], the bond lengths of Ni−Ni bonds for Ni_n/SV-N123 (n = 2, 3, 4) are 2.32 Å, 2.27 Å and 2.35 Å

respectively, which is closed to the calculation in this study.

3.2. Adsorption of NO molecule on Ni_n/SV-GS

In order to obtain the most stable geometries of NO adsorbed on the Ni clusters doped on various substrates. Vertical and horizontal NO gas molecules at different positions on the surface of substrates are optimized, and the most stable adsorbed geometries are shown in Fig. 2. The adsorption configuration of NO on the graphene-based supports is similar. It prefers N atom to bond with Ni_n metal clusters, and O atoms bond with N atoms, pointing to Ni_n metal clusters.
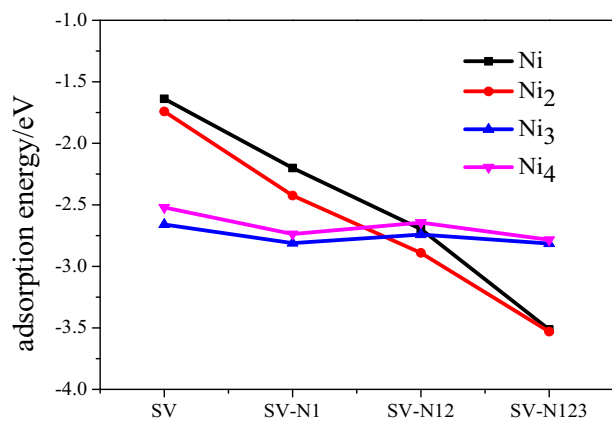
Fig. 3. The adsorption energy of NO on sixteen Ni_n/GS catalysts.

In order to clearly observe the adsorption effect of NO adsorbed on Ni_n/SV-GS, the most stable adsorption configuration was taken as the research object, and the broken-line diagram of adsorption energy of different support on NO was drawn, as shown in Fig. 3. It can be seen from the graph that the adsorption energy of Ni_n clusters (n = 1, 2) decreases gradually with the increase of nitrogen doping in graphene, while that of Ni clusters (n = 3, 4) decreases first, then increases and finally decreases with the increase of nitrogen doping in graphene. Among them, the structure of Ni_n/SV-N123 (n = 1, 2, 3 and 4) has the largest adsorption energy, which shows that the structure of Ni_n/SV-N123 has the best adsorption effect on NO. And for the structure of Ni_n/SV-N123, the adsorption energy of Ni/SV-N123 and Ni_2/SV-N123 is relatively large.

Liu et al. [29] found that there was a positive correlation between the charge of the Pt atom and the adsorption energy of Pt/GN catalyst. Gao et al. [40] also concluded that the charge quantity of Fe atom is also positively related to the adsorption energy of Fe/SV-GS surface. Like the above findings, we found that among all the Ni atoms in the Ni cluster, only the nearest Ni atom to graphene has the greatest charge transfer. By comparing the amount of charge carried by Ni atom with the adsorption energy of Pt/GN catalyst surface as shown in Fig. 4. When n = 1 and 2, the charge of Ni atom has a positive correlation with the adsorption energy of NO on Ni_n/SV-GS surface, and the square of the correlation coefficient are 0.91and 0.85 respectively, indicating that the adsorption of NO on Ni/SV-GS surface is mainly affected by the charge of Ni atom; but when n = 3 and 4, the correlation coefficient is

very low, indicating that when the number of atoms in the cluster increases, the adsorption of NO on the surface of Ni/SV-GS may be influenced by other factors.

Due to the increase of the number of Ni atoms in the Ni clusters and the interaction between each Ni atoms, the adsorption energy of NO on the Ni_n/SV-GS surface may be positively correlated with the average bond length between the Ni atoms. As shown in Fig. 5, the adsorption energy is strongly positively correlated with the average length of Ni−Ni bond, and the square of the correlation coefficient is 0.88 and 0.86 respectively. So the average length of Ni−Ni bond can explain the low of the adsorption energy (n = 3 and 4). The adsorption energy of Ni clusters and graphene (E_{ads}, eV), the charge of the Ni_1 after adsorption (q_1, e) and the average bond length of Ni−Ni bonds after adsorption (d_{Ni-Ni}, Å) are summarized in Table S1.

Overall, The adsorption energy of Ni clusters (n = 1, 2) decreases gradually with the increase of nitrogen doping in graphene, because of the effect of the charge of Ni atom; while the adsorption energy of Ni clusters (n = 3, 4) decreases first, then increases and finally decreases with the increase of nitrogen doping in graphene, because of the influence of the average length of Ni−Ni bond. And there is an issue that needs to be further discussed: the relationship between the support effect of different catalyst structures (Ni_n/SV-GS) and the adsorption energy of NO. In order to analyze this issue, the electronic properties analysis, the density of states and the Fermi softness analysis have been performed.

3.3. Electronic properties analysis

To further analyze the electronic characteristics of NO adsorption, the electron transfer is calculated, as shown in Table 2. It is shown that NO is mainly obtained electrons in the process of NO adsorption under various structures. It is indicated that the support effect has a great influence on the adsorption of NO. For different catalyst structures (Ni_n/SV-GS), the charge and corresponding charge transfer of each atom are different. In addition, there is no obvious linear relationship between the NO gas charge transfer and the adsorption energy. We have plotted electron density difference of NO adsorption on the substrate in Fig. 6, Electron density difference (EDD) is calculated by the difference between the charge density of the whole structure after the bond and the charge density of the corresponding two isolated systems, which are the NO and the Ni_n/Fe/SV-GS. The EDD is defined as: $\Delta\rho = \rho_{NO-Ni_n/SV-GN} - \rho_{NO} - \rho_{Ni_n/SV-GN}$. Charge shifts, resonance character and bonding polarization directions in the process of bonding and bonding electron coupling can be clearly obtained.

(a) $n=1$

$E_{ads} = 11.48\ q - 108.63$

$R^2 = 0.91$

(b) $n=2$

$E_{ads} = 5.59\ q - 55.19$

$R^2 = 0.85$
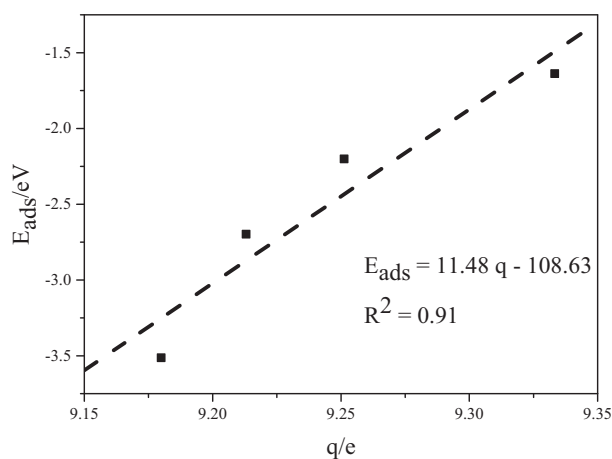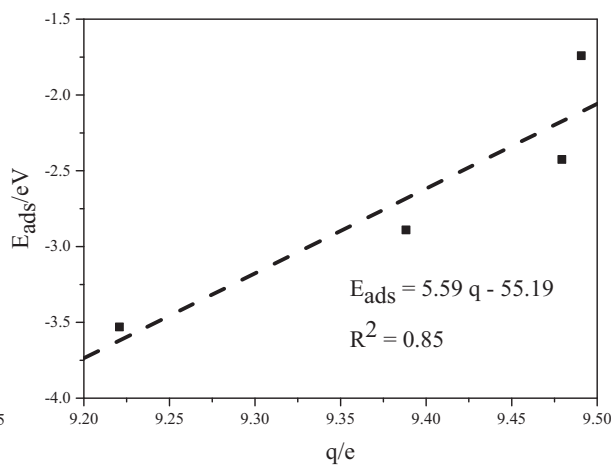
Fig. 4. The adsorption energy of NO as a function of the charge of the Ni atom.
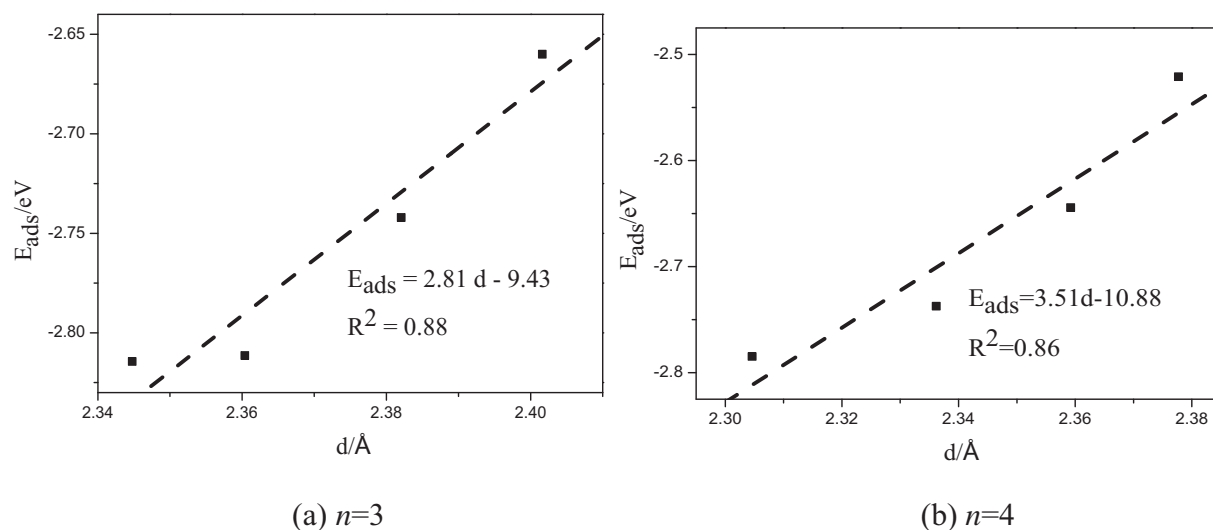
(a) *n*=3

(b) *n*=4

Fig. 5. The adsorption energy of NO as a function of the average of Ni−Ni bond length.

Table 2
The charge transfer of NO gas molecules on sixteen Ni_n/GS catalysts.

Δq-gas (e)	SV-GN	SV-N1	SV-N12	SV-N123
Ni	0.322	0.302	0.321	0.331
Ni_2	0.308	0.310	0.311	0.518
Ni_3	0.517	0.498	0.264	0.649
Ni_4	0.263	0.278	0.280	0.333

As shown in Fig. 6, cyan represents electron loss and yellow represents electron gain. The NO gas is mainly surrounded by yellow color, and the Ni_n clusters are mainly surrounded by cyan color, indicating that the charge density can transfer from the Ni_n clusters to NO gas molecules during adsorption. This is the same as the result of the previous bader charge analysis. The corresponding EDD diagram also

shows that the electron density rearrangement occurs during the formation of complexes. There is a yellow overlap between the N atoms of NO molecule and Ni atoms of Ni clusters in Fig. 6, indicating a strong combination of N atoms and Ni atoms.

3.4. Density of states of NO on Ni_n/SV-GS

In order to study the support effect of Ni_n/SV-GS toward NO, the projected density of states (PDOS) of NO on Ni_n/SV-GS is plotted, as shown in Figs. 7–10. The DOS is used to explain the number of states that can be occupied by electrons at each level. The PDOS is calculated to provide the contribution of each band to a given atomic orbitals. The d orbit of Ni atom and the p orbit of N atom in NO gas molecule are shown in Figs. 7–10. The dashed line and the solid line represent the PDOS of NO gas before and after adsorption, respectively. In Figs. 7–10,
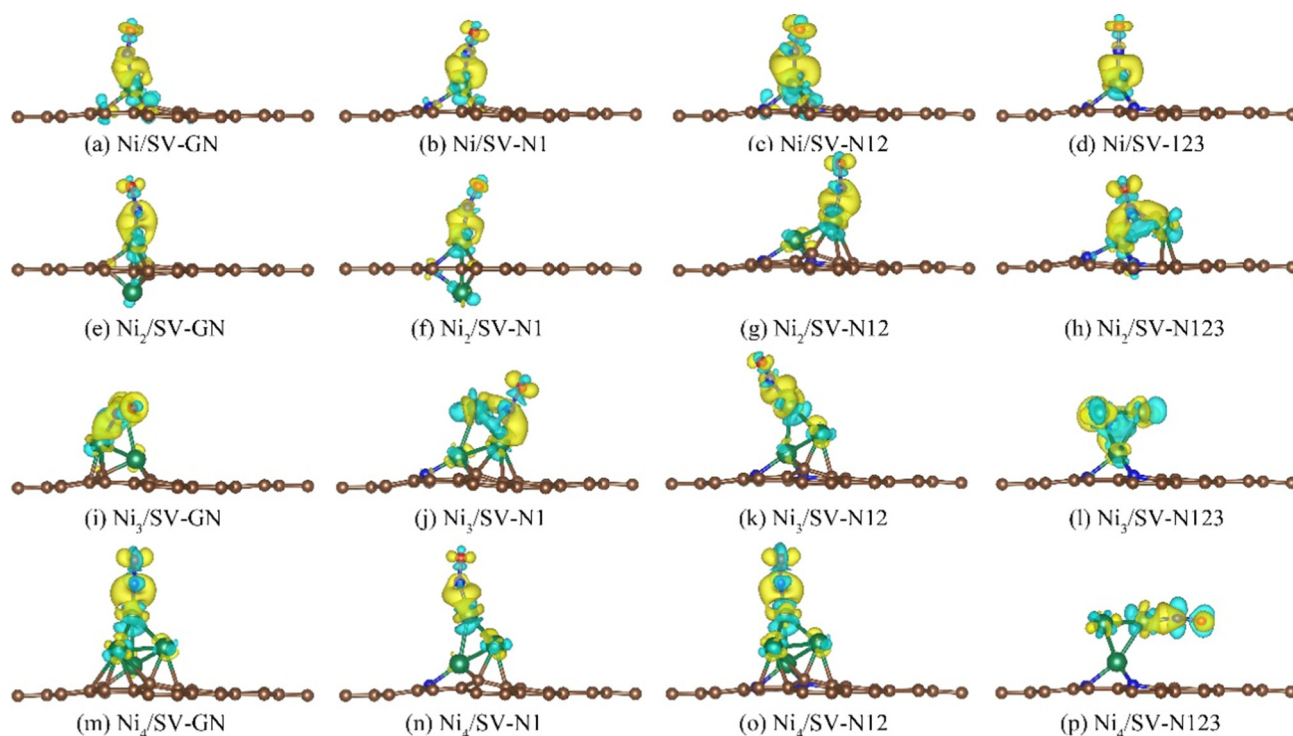

Fig. 6. The electron density difference of NO molecule adsorbs on Ni_n/SV-GS. (The contour lines in plots are drawn at 0.005 e/Å intervals).
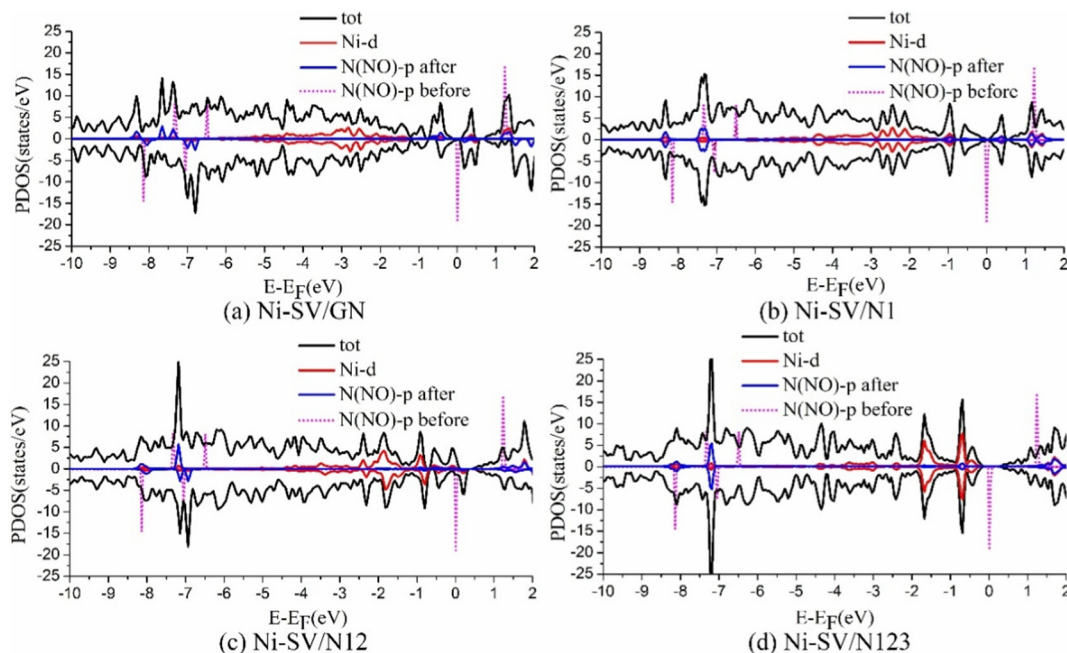
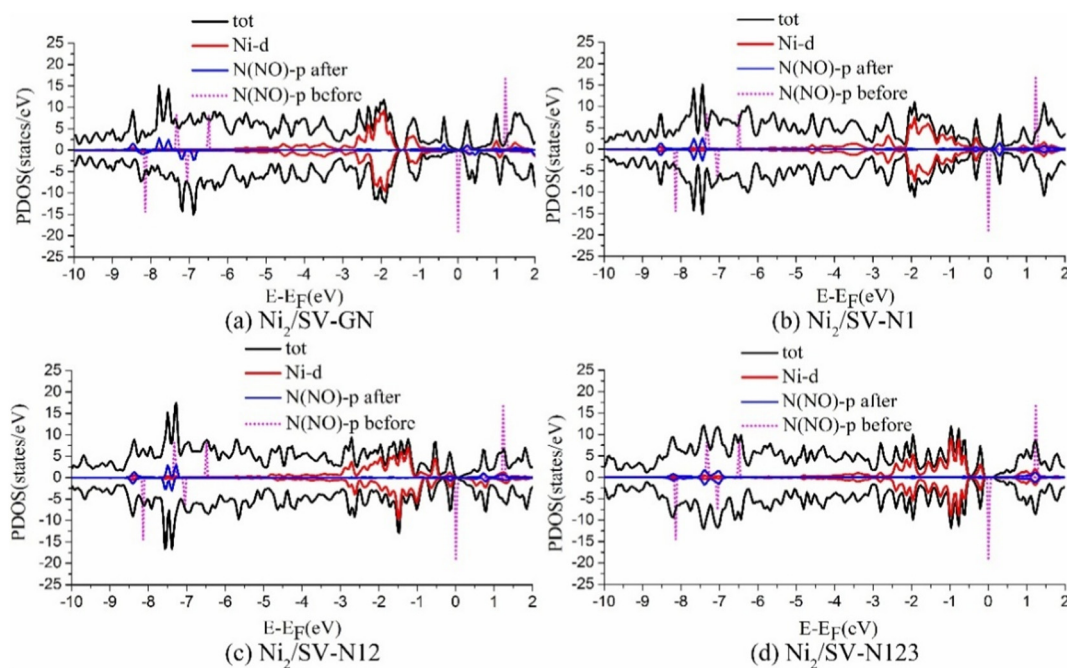**Fig. 7.** The PDOS of NO molecule adsorbs on Ni/SV-GS.

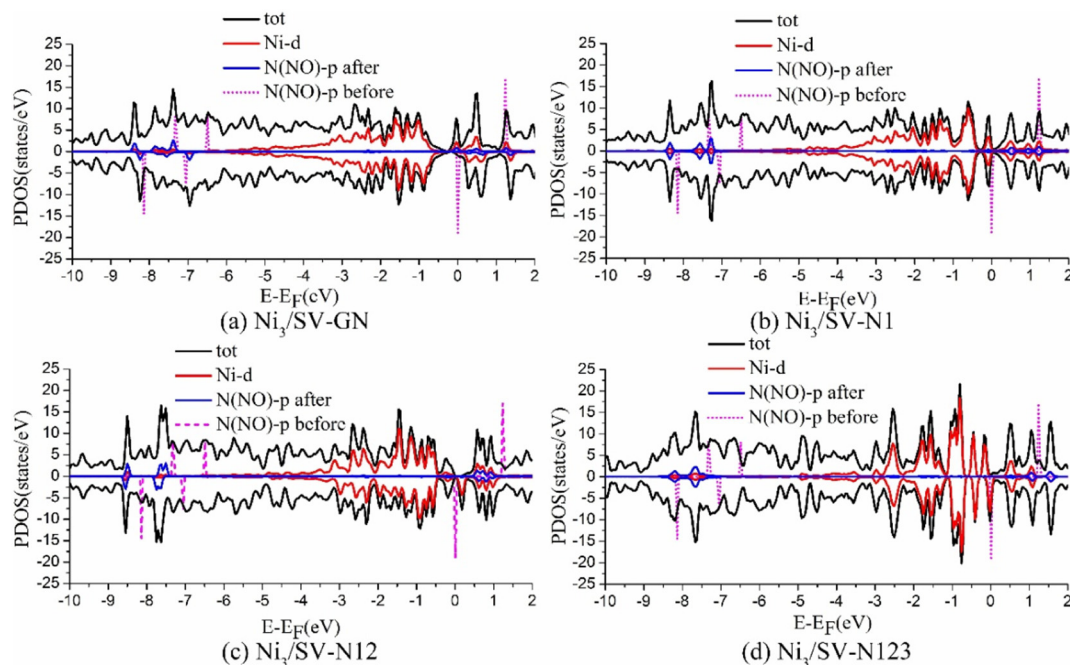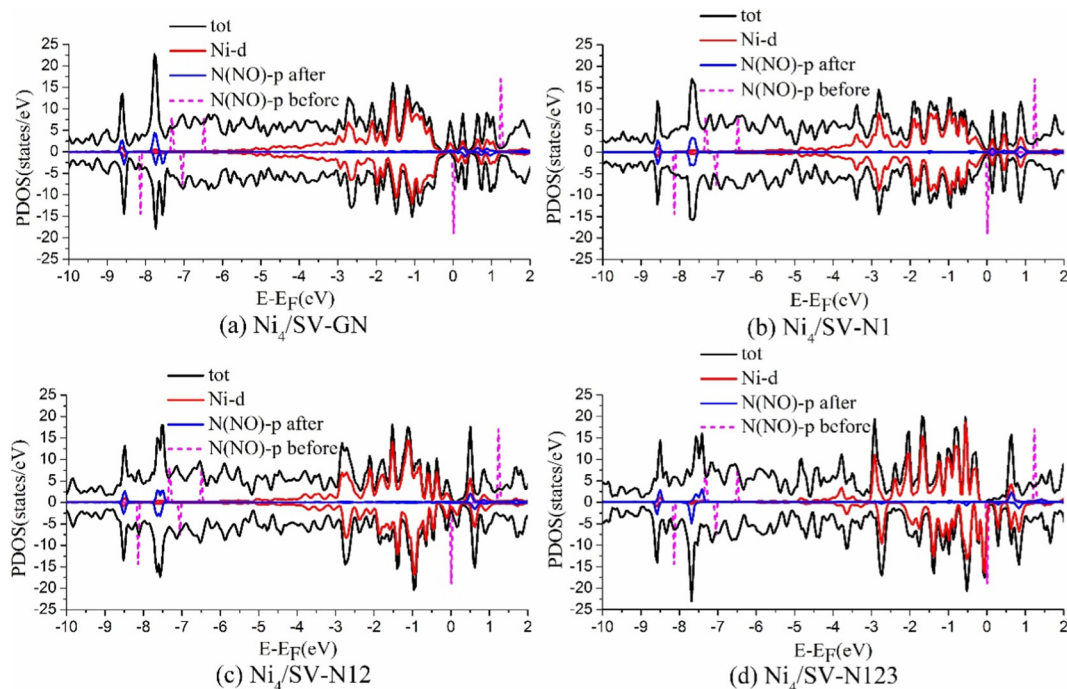**Fig. 8.** The PDOS of NO molecule adsorbs on Ni_2/SV-GS.

it is shown that the *p* orbit sharp peaks of N atoms of NO is 1.24 eV before the NO gas molecule adsorbed in Ni_n/SV-GS. In addition, the *p* orbit of the N atom is shifted down to a lower energy states when NO is adsorbed on the substrate. For the NO-Ni_n/SV-GS system, the *d*-states of Ni atoms overlap with *p*-states of N atoms of NO near the Fermi level. As the size of the Ni clusters increases, the PDOS of N atoms of NO change negligibly for each of graphene-based substrates. Nevertheless, the peak of d orbit of Ni atom increases and moves toward the Fermi level simultaneously, which shows a strong hybridization in the N-2*p* orbitals and Ni-3*d* orbitals.

According to the previous article, the *d* orbital of the metal atom in TM/GS played a great role in the adsorption and reaction processes. From the definition of density of states, the greater value of a certain

energy level, the greater charge density at that energy level. In order to find the role of *d* orbit of Ni atom in the adsorption of NO on the substrate, the area of *d* orbit of the Ni atom from −6 to 0 eV occupies the proportion of the area of total density of states is calculated, as shown in Table 3. The greater the proportion is, the greater the role of Ni atoms in the NO adsorption process is. It is shown that the proportion of Ni *d* band is larger with the increase of the number of Ni atoms. In other words, with the increase of the number of Ni atoms in Ni_n/GS-SV, Ni atom plays a more and more vital role in NO adsorption process.

3.5. Electronic structure analysis

As mentioned above, the difference of the adsorption energy of NO

Fig. 9. The PDOS of NO molecule adsorbs on Ni_3/SV-GS.

Fig. 10. The PDOS of NO molecule adsorbs on Ni_4/SV-GS.

Table 3
The proportion of d orbit to total density of states.

Proportion (%)	SV-GN	SV-N1	SV-N12	SV-N123
Ni	14.6	14.8	14.4	15.1
Ni_2	27.8	27.5	29.3	27.5
Ni_3	35.9	35.6	35.5	37.1
Ni_4	41.6	42.1	42.9	42.4

on Ni_n/SV-GS is mainly due to the difference of the graphene-based supports. The effect of graphene based carrier is closely related to the electronic structure. In order to further study the intrinsic relationship between support effect and the electrical structure of Ni_n/SV-GN catalyst, this paper will analyze from two aspects: d-band center and Fermi softness. The d-band center (ε_d) of Ni_n/SV-GS were calculated as follows:

$$\varepsilon_d = \frac{\int_{-\infty}^{+\infty} E \cdot D(E) dE}{\int_{-\infty}^{+\infty} D(E) dE}$$

(4)

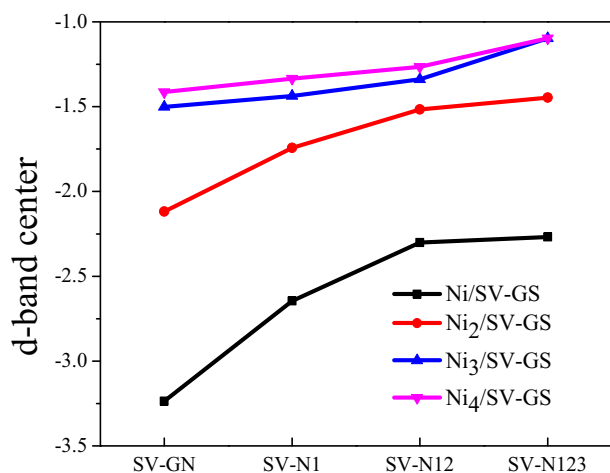where $D(E)$ is the d-states of Ni atom in Ni_n/SV-GN catalysts.

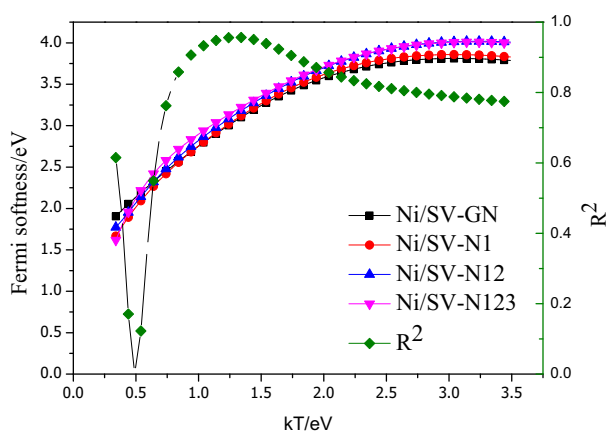Fig. 11. The d-band center of different Ni_n/GS.

Fig. 12. The effect of different kT on Fermi softness and correlation coefficient of Ni.
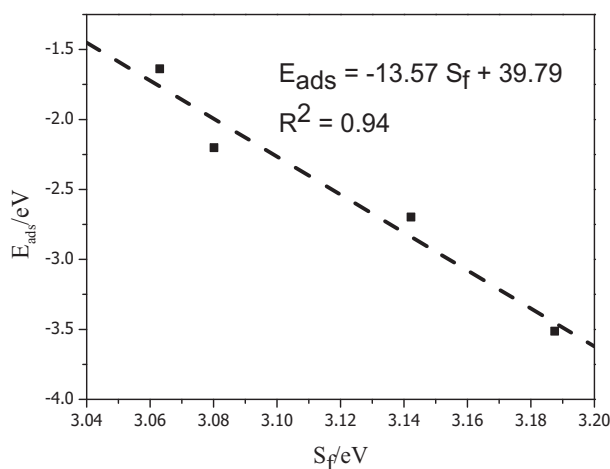

Fig. 13. The adsorption energy of NO as a function of Fermi softness using $kT = 1.30$ eV.
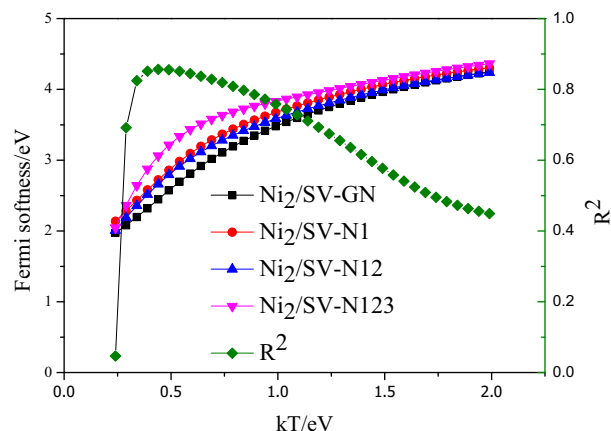

Fig. 14. The effect of different kT on Fermi softness and correlation coefficient of Ni_2.

center is close to zero too.

According to frontier molecular orbital theory, the whole frontier electronic band of the solid surface is reactive. It is known that the closer the electronic state to the Fermi level, the greater the contribution to bonding interaction. Therefore, the reactivity of a catalyst should be determined by both the density of states ($g(E)$) and a weight function ($W(E)$) which quantifies the contribution of every electronic state to the surface bonding. Recently, Zhuang et al. [42] proposed a new property, Fermi softness (S_F), which accurately and quantitatively describes the chemical reactivity of solid surfaces. The core idea is to create a reactive weight function at the maximum Fermi level, so as to determine the weighted sum of the density of state on the solid surface, and the S_F can be calculated from the following equation:

$$S_F = - \int_{-\infty}^{+\infty} g(E) \cdot W(E) dE \tag{5}$$

where $g(E)$ is the total density of states. $W(E)$ can be acquired from the derivative of the Fermi-Dirac function, $-f_T'(E - E_F)$.

The $-f_T'(E - E_F)$ is calculated as the following equation:

$$-f_T'(E - E_F) = \frac{1}{kT} \cdot \frac{1}{\left(e^{\frac{E-E_F}{kT}} + 1\right)\left(e^{\frac{E_F-E}{kT}} + 1\right)} \tag{6}$$

where kT is the nominal electron temperature (k is the Boltzmann constant and T is the parametric temperature).

The method successfully reveals the fine reactive structure of many complex catalyst surfaces and the spatial anisotropic catalytic properties of the chemical reaction. Although Fermi softness has been proved to be a good descriptor of the reactivity on solid surfaces, and there is no other theory to achieve its unique function, but Fermi softness in the cluster catalyst system is rarely studied. Hence, we apply the Fermi softness in Ni_n clusters catalyst system. According to the research Zhuang [42] proposed calculating Fermi's softness, the value of kT between different adsorption systems are different. So it is necessary to choose an appropriate value of kT before applying the Fermi softness to analyze the activity of the catalyst.

In order to obtain the optimal value of kT and study the effect of kT on Fermi softness, we calculated the Fermi softness of $Ni_n/SV-GS$ with different kT. Firstly, we calculated the correlation between the adsorption energy of NO and Fermi softness with different kT. The Fermi softness of Ni/SV-GS and the correlation coefficient (R^2) with different kT were drawn, as shown in Fig. 12. The value of Fermi softness changes significantly with the increase of kT. When kT is > 0.5 eV, the correlation coefficient (R^2) between Fermi softness and adsorption energy increases first and then decreases with the increase of kT. When the $kT = 1.30$ eV, the correlation coefficient (R^2) reaches its the maximum (0.94), and the S_F of Ni/SV-GN, Ni/SV-N1, Ni/SV-N12 and Ni/

Gorzkowski et al. [41] found that the d band center has a great relationship with the catalyst activity. Then, we use formula (4) to calculate the d-band center. The d-band center of different $Ni_n/SV-GS$ is shown in Fig. 11, it can be found that for any Ni_n cluster, with the increase of N doping number, the d-band center is closer to zero. In addition, with the number of Ni in the Ni cluster increasing, the d-band
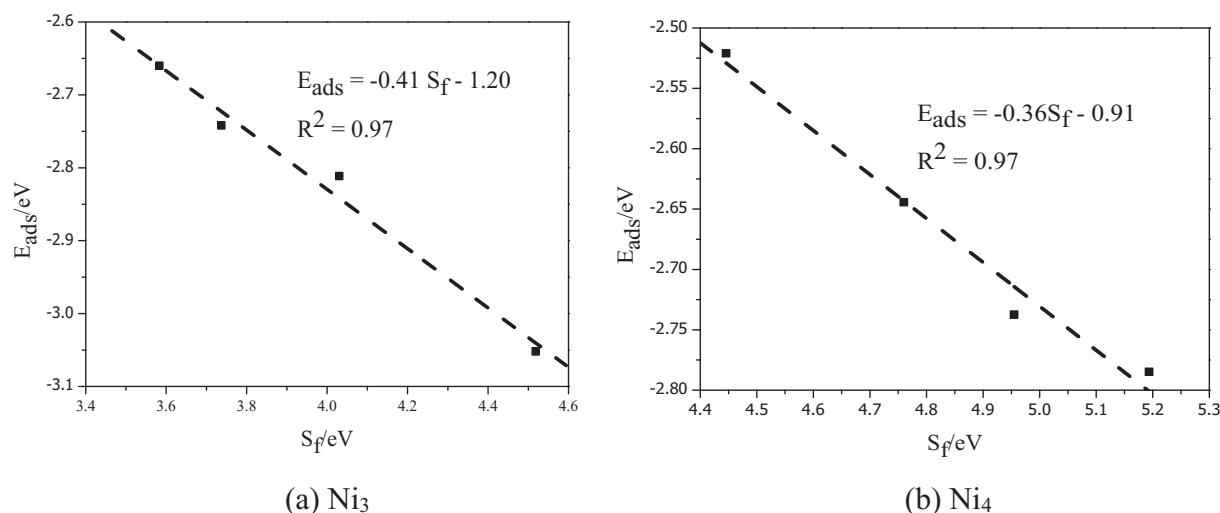
(a) Ni$_3$ (b) Ni$_4$

Fig. 15. The adsorption energy of NO as a function of Fermi softness using $kT = 0.45$ eV.

SV-N123 is 3.03 eV, 3.08 eV, 3.14 eV and 3.19 eV, respectively. It is different to NO adsorbed on Fe single atom catalyst ($kT = 0.15$ eV) calculated by the previous reported results [43]. Because the two single atom catalysts are loaded with different metal atoms (Fe and Ni), the kT of the two single atom catalysts are different. It can be found obvious linear relationship through linear fitting of adsorption energy and Fermi softness at $kT = 1.30$ eV, as shown in Fig. 13. In addition, the research results show that Fermi softness is a new descriptor to characterize the adsorption activity of Ni/SV-GS catalyst system.

Then, we calculated the correlation between the adsorption energy of NO ($n = 2, 3$ and 4) and Fermi softness with $kT = 1.30$ eV, but the correlation coefficient (R^2) is very small. It is indicated that the optimal value of kT of Ni/SV-GS catalyst is unsuited the cluster catalyst system. So we calculated the correlation between the adsorption energy of Ni$_2$/SV-GS and Fermi softness with different kT. The Fermi softness of Ni$_2$/SV-GS and the correlation coefficient (R^2) with different kT were drawn, as shown in Fig. 14. The correlation coefficient (R^2) between Fermi softness and adsorption energy increases first and then decreases with the increase of kT. When the $kT = 0.45$ eV, the correlation coefficient (R^2) reaches its the maximum (0.86), and the S_F of Ni$_2$/SV-GN, Ni$_2$/SV-N1, Ni$_2$/SV-N12 and Ni$_2$/SV-N123 is 2.47 eV, 2.75 eV, 2.69 eV and 3.10 eV, respectively. It is different from the single atom nickel catalyst system ($kT = 1.30$ eV). This is mainly due to the difference between graphene based single atom catalysts and graphene based nanocluster catalysts.

In order to further provide the correlation between Fermi softness and adsorption energy, the correlation lines between adsorption energy of Ni$_n$ ($n = 3, 4$) and Fermi softness are plotted, as shown in Fig. 15. In Fig. 15, it is clearly shown that there is a high negative correlation between the adsorption energy of Ni$_n$ ($n = 3, 4$) and Fermi softness and the correlation coefficient between the adsorption energy of Ni$_n$ ($n = 3, 4$) and the correlation coefficient (R^2) are 0.97 and 0.97, respectively. The Fermi softness quantifies the contribution of every electronic state to the surface bonding. The larger the value of a certain catalyst Fermi, the higher the reactivity of the catalyst, and the correction between Fermi softness of Ni$_n$/SV-GS and the adsorption of NO is high. So the density of states and the Fermi softness analyzes the influence mechanism of the support effect on the adsorption from the electronic structure perspective.

4. Conclusion

Through comprehensive and systematic research of the adsorption of NO on Ni$_n$ cluster doped graphene with different graphene-based support, the adsorption configuration, adsorption energy, charge transfer and density of states of NO on Ni$_n$/graphene ($n = 1, 2, 3$ and 4) are thoroughly studied and the d-band center and Fermi softness has been performed to consider the support effect. It is indicated that the support effect has a significant effect on the adsorption characteristics of NO molecules, which depends on the electronic structure of graphene-based support. The electronic structure can be characterized by the Fermi softness of the catalyst. The adsorption energy of Ni clusters ($n = 1, 2$) decreases gradually with the increase of nitrogen doping in graphene, while the adsorption energy of Ni clusters ($n = 3, 4$) decreases first, then increases and finally decreases with the increase of nitrogen doping in graphene. The largest adsorption energy is the Ni$_n$/SV-N123, which are used as a good catalyst for NO gas. Ni atom plays a more and more important role in NO adsorption process, with the increase of the number of Ni atoms. The Fermi softness is a great descriptors for the adsorption activity of the Ni$_n$/SV-GS. We hoped that this work will provide a more in-depth and systematic understanding of cluster doped graphene-based support catalysts and play a guiding role in the design of metal nanoparticles catalysts for the adsorption of NO.

Supplementary data to this article can be found online at https://doi.org/10.1016/j.apsusc.2019.03.186.

References

[1] E.D. Amster, M. Haim, J. Dubnov, D.M. Broday, Contribution of nitrogen oxide and sulfur dioxide exposure from power plant emissions on respiratory symptom and disease prevalence, Environ. Pollut. 186 (2014) 20–28.
[2] H. Tian, K. Liu, J. Hao, Y. Wang, J. Gao, P. Qiu, C. Zhu, Nitrogen oxides emissions from thermal power plants in China: current status and future predictions, Environ. Sci. Technol. 47 (2013) 11350–11357.
[3] V.S. Guido Saracco, Simultaneous removal of nitrogen oxides and fly-ash from coal-based power-plant flue gases, Appl. Therm. Eng. (1998) 1025–1035.
[4] D. Yang, Q.W. Chen, The discharge status and technical analysis of NOX of thermal power plant boiler, Appl. Mech. Mater. 535 (2014) 131–134.
[5] M.S. Maqbool, A.K. Pullur, H.P. Ha, Novel sulfation effect on low-temperature activity enhancement of CeO2-added Sb-V2O5/TiO2 catalyst for NH3-SCR, Appl. Catal. B Environ. 152-153 (2014) 28–37.
[6] H. Chang, X. Chen, J. Li, L. Ma, C. Wang, C. Liu, J.W. Schwank, J. Hao,

Improvement of activity and SO(2) tolerance of Sn-modified MnOx-CeO(2) catalysts for NH(3)-SCR at low temperatures, Environ. Sci. Technol. 47 (2013) 5294–5301.

[7] J. Szanyi, J.H. Kwak, H. Zhu, C.H. Peden, Characterization of Cu-SSZ-13 NH3 SCR catalysts: an in situ FTIR study, Phys. Chem. Chem. Phys. 15 (2013) 2368–2380.

[8] W. Chen, Z. Qu, W. Huang, X. Hu, N. Yan, Novel effect of SO2 on selective catalytic oxidation of slip ammonia from coal-fired flue gas over IrO2 modified Ce–Zr solid solution and the mechanism investigation, Fuel 166 (2016) 179–187.

[9] X. Gao, Z. Du, H.-l. Ding, Z.-l. Wu, H. Lu, Z.-y. Luo, K.-f. Cen, Kinetics of NOx absorption into (NH4)2SO3 solution in an ammonia-based wet flue gas desulfurization process, Energy Fuel 24 (2010) 5876–5882.

[10] S. Dobrin, CO oxidation on Pt nanoclusters, size and coverage effects: a density functional theory study, Phys. Chem. Chem. Phys. 14 (2012) 12122–12129.

[11] L. Guo, R. Zhang, L.L. Guo, S. Niu, CO oxidation on subnanometer AlPtn clusters, Computational and Theoretical Chemistry 1036 (2014) 7–15.

[12] X. Lian, W. Guo, F. Liu, Y. Yang, P. Xiao, Y. Zhang, W. Tian, DFT studies on Pt 3 M (M = Pt, Ni, Mo, Ru, Pd, Rh) clusters for CO oxidation, Comput. Mater. Sci. 96 (2015) 237–245.

[13] B.M. Weiss, E. Iglesia, NO oxidation catalysis on Pt clusters: elementary steps, structural requirements, and synergistic effects of NO2 adsorption sites, J. Phys. Chem. C 113 (2009) 13331–13340.

[14] J. Wei, Z. Zang, Y. Zhang, M. Wang, J. Du, X. Tang, Enhanced performance of light-controlled conductive switching in hybrid cuprous oxide/reduced graphene oxide (Cu < sub > 2 < /sub > O/rGO) nanocomposites, Opt. Lett. 42 (2017) 911–914.

[15] X. Liu, T. Xu, Y. Li, Z. Zang, X. Peng, H. Wei, W. Zha, F. Wang, Enhanced X-ray photon response in solution-synthesized CsPbBr3 nanoparticles wrapped by reduced graphene oxide, Sol. Energy Mater. Sol. Cells 187 (2018) 249–254.

[16] Z. Zang, X. Zeng, M. Wang, W. Hu, C. Liu, X. Tang, Tunable photoluminescence of water-soluble AgInZnS–graphene oxide (GO) nanocomposites and their application in-vivo bioimaging, Sensors Actuators B Chem. 252 (2017) 1179–1186.

[17] T. Gao, S. Xie, Y. Gao, M. Liu, Y. Chen, Y. Zhang, Z. Liu, Growth and atomic-scale characterizations of graphene on multifaceted textured Pt foils prepared by chemical vapor deposition, ACS Nano 5 (2011) 9194–9201.

[18] M. Liu, Y. Zhang, Y. Chen, Y. Gao, T. Gao, D. Ma, Q. Ji, Y. Zhang, C. Li, Z. Liu, Thinning segregated graphene layers on high carbon solubility substrates of rhodium foils by tuning the quenching process, ACS Nano 6 (2012) 10581–10589.

[19] K.S. Novoselov, Graphene: materials in the flatland, Int. J. Mod. Phys. B 25 (2011) 4081–4106.

[20] W. Wu, Q. Yu, P. Peng, Z. Liu, J. Bao, S.S. Pei, Control of thickness uniformity and grain size in graphene films for transparent conductive electrodes, Nanotechnology 23 (2012) 035603.

[21] K. Koizumi, K. Nobusada, M. Boero, Reducing the cost and preserving the reactivity in noble-metal-based catalysts: oxidation of CO by Pt and Al–Pt alloy clusters supported on graphene, Chemistry 22 (2016) 5181–5188.

[22] Y. Tang, Z. Lu, W. Chen, W. Li, X. Dai, Geometric stability and reaction activity of Pt clusters adsorbed graphene substrates for catalytic CO oxidation, Phys. Chem. Chem. Phys. 17 (2015) 11598–11608.

[23] S. Amaya-Roncancio, A.A. García Blanco, D.H. Linares, K. Sapag, DFT study of hydrogen adsorption on Ni/graphene, Appl. Surf. Sci. 447 (2018) 254–260.

[24] D. Farmanzadeh, T. Abdollahi, H2 adsorption on free and graphene-supported Ni nanoclusters: a theoretical study, Surf. Sci. 668 (2018) 85–92.

[25] H. Xu, W. Chu, W. Sun, C. Jiang, Z. Liu, DFT studies of Ni cluster on graphene surface: effect of CO2 activation, RSC Adv. 6 (2016) 96545–96553.

[26] A.W. Robertson, B. Montanari, K. He, J. Kim, C.S. Allen, Y.A. Wu, J. Olivier, J. Neethling, N. Harrison, A.I. Kirkland, J.H. Warner, Dynamics of single Fe atoms in graphene vacancies, Nano Lett. 13 (2013) 1468–1475.

[27] M.A.N. Dewapriya, R.K.N.D. Rajapakse, Effects of free edges and vacancy defects on the mechanical properties of graphene, in: IEEE International Conference on Nanotechnology, 2014, pp. 908–912.

[28] F. Banhart, J. Kotakoski, A.V. Krasheninnikov, Structural defects in graphene, ACS Nano 5 (2011) 26–41.

[29] S. Liu, S. Huang, Theoretical insights into the activation of O2 by Pt single atom and Pt4 nanocluster on functionalized graphene support: critical role of Pt positive polarized charges, Carbon 115 (2017) 11–17.

[30] K. G., F. J., Efficient iterative schemes for ab initio total-energy calculations using a plane-wave basis set, Phys. Rev. B Condens. Matter, 54 (1996) 11169–11186.

[31] G. Kresse, J. Furthmüller, Efficiency of ab-initio total energy calculations for metals and semiconductors using a plane-wave basis set, Comput. Mater. Sci., 6 (1996) 15–50.

[32] G. Kresse, D. Joubert, From ultrasoft pseudopotentials to the projector augmented-wave method, Phys. Rev. B 59 (1999) 1758–1775.

[33] B. Burke, Generalized gradient approximation made simple, Phys. Rev. B 77 (1996) 3865–3868.

[34] P. J.P., B. K., E. M., Generalized gradient approximation made simple, Phys. Rev. Lett., 77 (1996) 3865–3868.

[35] M.D. Esrafili, F. Sharifi, L. Dinparast, Catalytic hydrogenation of CO2 over Pt- and Ni-doped graphene: a comparative DFT study, J. Mol. Graph. Model. 77 (2017) 143–152.

[36] S. Gholami, A. Shokuhi Rad, A. Heydarinasab, M. Ardjmand, Adsorption of adenine on the surface of nickel-decorated graphene; a DFT study, J. Alloys Compd. 686 (2016) 662–668.

[37] X.-Y. Xu, J. Li, H. Xu, X. Xu, C. Zhao, DFT investigation of Ni-doped graphene: catalytic ability to CO oxidation, New J. Chem. 40 (2016) 9361–9369.

[38] X. Zhou, W. Chu, W. Sun, Y. Zhou, Y. Xue, Enhanced interaction of nickel clusters with pyridinic-N (B) doped graphene using DFT simulation, Computational and Theoretical Chemistry 1120 (2017) 8–16.

[39] C.M. Ramos-Castillo, J.U. Reveles, M.E. Cifuentes-Quintal, R.R. Zope, R. de Coss, Ti4- and Ni4-doped defective graphene nanoplatelets as efficient materials for hydrogen storage, J. Phys. Chem. C 120 (2016) 5001–5009.

[40] Z.Y. Gao, W.J. Yang, X.L. Ding, G. Lv, W.P. Yan, Support effects on adsorption and catalytic activation of O2 in single atom iron catalysts with graphene-based substrates, Phys. Chem. Chem. Phys. 20 (2018) 7333–7341.

[41] M.T. Gorzkowski, A. Lewera, Probing the limits of d-band center theory: electronic and electrocatalytic properties of Pd-shell–Pt-core nanoparticles, J. Phys. Chem. C 119 (2015) 18389–18395.

[42] B. Huang, L. Xiao, J. Lu, L. Zhuang, Spatially resolved quantification of the surface reactivity of solid catalysts, Angew. Chem. Int. Ed. Eng. 55 (2016) 6239–6243.

[43] Z. Gao, Y. Sun, M. Li, W. Yang, X. Ding, Adsorption sensitivity of Fe decorated different graphene supports toward toxic gas molecules (CO and NO), Appl. Surf. Sci. 456 (2018) 351–359.